Translating planar heterocycles into 3D analogs via photoinduced hydrocarboxylation

Myriam Mikhael[†], Sara N. Alektiar[††], Charles S. Yeung*[†††], and Zachary K. Wickens*[††]
[†]MRL Postdoctoral Fellow, Discovery Chemistry, Merck & Co., Inc., Massachusetts 02115, United States
[††]Department of Chemistry, University of Wisconsin−Madison, Madison, Wisconsin 53706, United States
[†††]Discovery Chemistry, Merck & Co., Inc., Boston, Massachusetts 02115, United States

Abstract:

The rapid preparation of complex three-dimensional (3D) heterocyclic scaffolds is a key challenge in modern medicinal chemistry. Small molecule therapeutic candidates with increased 3D complexity, on average, possess a higher probability of clinical success. However, new drug targets remain dominated by flat molecules due the wealth of robust coupling reactions available for their construction. Heteroarene dearomatization reactions offer an ideal opportunity to transform readily accessible 2D structures into saturated analogs. Broadly employed heteroarene hydrogenation reactions rehybridize C(sp^2) sites to C(sp^3) without otherwise perturbing the molecular shape. In stark contrast, heteroarene difunctionalization strategies dramatically change the molecular structure. In principle, heteroarene hydrofunctionalization reactions constitute an elusive middle ground by disrupting aromaticity and introducing a single molecular vector. Unfortunately, dearomative hydrofunctionalization reactions remain limited. Herein, we report a new strategy to enable the dearomative hydrocarboxylation of indoles and related heterocycles. This reaction represents a rare example of a heteroarene hydrofunctionalization that meets the numerous requirements for broad implementation in drug discovery. The transformation is highly chemoselective, broad in scope, operationally simple, and readily amenable to high-throughput experimentation (HTE). Accordingly, this process will allow existing libraries of heteroaromatic compounds to be translated into diverse 3D analogs and enable exploration of new classes of medicinally relevant molecules.

MAIN: Interrogation of increasingly complex 3D target molecules has emerged as a central goal in drug discovery chemistry. A recent meta-analysis of biologically active molecules proceeding through clinical trials established that success of these candidates correlates well with their 3D complexity.[1,2] However, the robust coupling reactions regularly employed in medicinal chemistry disproportionately produce C(sp^2) linkages.[3,4] Consequently, flat molecules remain overrepresented in new clinical candidates despite the enhanced bioactivities and decreased side-effects observed from molecules with an increased degree of saturation.[1,2,5] Dearomatization reactions unlock an approach to directly convert these synthetically accessible planar scaffolds into more C(sp^3)–rich congeners.[6–8] Indeed, heteroarene hydrogenation reactions are regularly employed to deliver medicinally-relevant saturated or partially-saturated heterocyclic motifs from widely available heteroaromatic starting materials.[9–11] In principle, heteroarene hydrofunctionalization constitutes a deceptively simple class of complementary dearomatization reactions (Fig 1A). These transformations disrupt planarity while also installing a new molecular vector. Accordingly, a general approach to heteroarene hydrofunctionalization would enable rapid integration of more three-dimensionally complex molecular targets. While substantial progress has been made in heteroarene hydrogenation, hydrofunctionalization processes remain difficult. In the context of basic heterocycles (*e.g.* pyridine and quinoline derivatives), the Lewis basic nitrogen provides an avenue to transform the heteroarene into an electrophile and has enabled progress in hydrofunctionalization. However, this approach is not feasible for electron rich heterocycles (*e.g.* indole and benzofuran derivatives), and accordingly hydrofunctionalization of these molecules has remained dominated by intramolecular approaches and harsh conditions.[12–16] Unfortunately, implementation of a heteroarene hydrofunctionalization strategy in drug discovery imposes numerous additional design constraints beyond the energetic demands underpinning any dearomatization process. The reaction must be (1) mild and functional group tolerant, (2) reliable and operationally simple, and (3) chemoselective for specific sites in heterocyclic moieties in the presence of the other (hetero)arenes. Ideally, the process would also be amenable to high-throughput experimentation (HTE) to allow parallel library synthesis.

Fig. 1: Project overview and reaction development

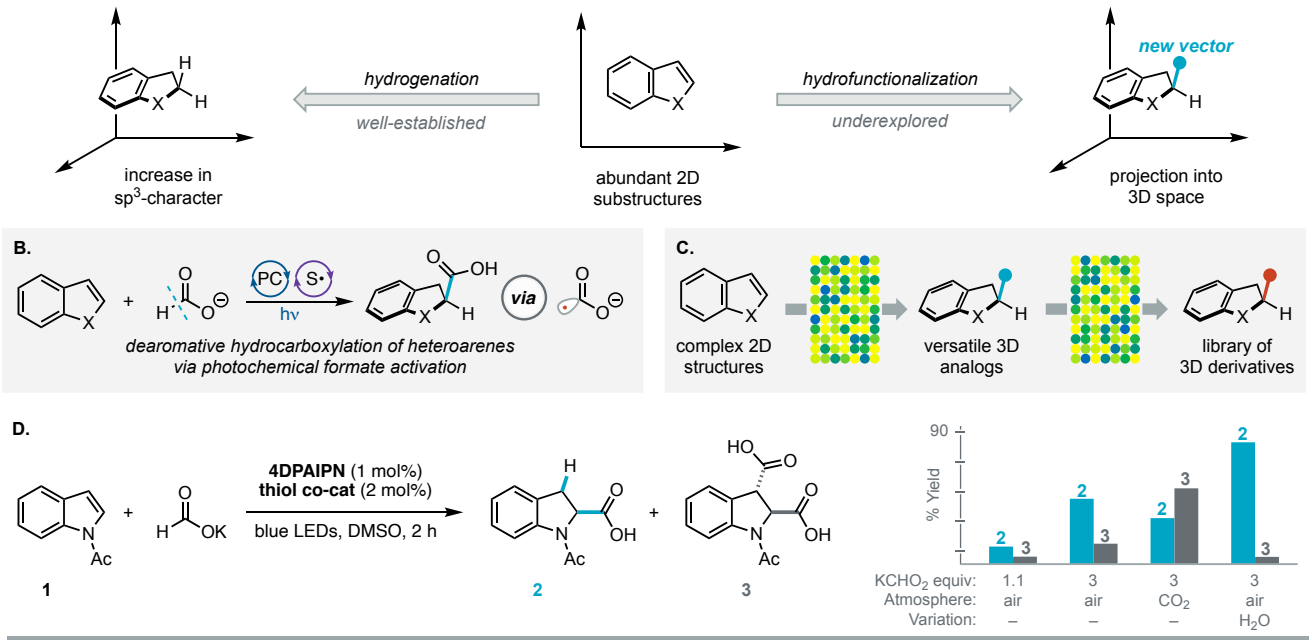

a, Installation of a new 3D vector via ideal hydrofunctionalization reaction. **b**, Our proposed dearomative hydrocarboxylation reaction involving the coupling of heteroarenes with formate via a $CO_2^{\bullet-}$ intermediate. **c**, Rapid diversification of planar structures via high-throughput experimentation. **d**, Development of our photoinitiated hydrocarboxylation reaction. Reactions were conducted on a 0.05 mmol scale and yields were determined by ^{1}H-NMR. See *Supporting Information* for further details.

We questioned whether direct hydrocarboxylation of indoles and related heterocycles could be accomplished under sufficiently mild conditions to serve as a general platform for heteroarene hydrofunctionalization (Fig 1B). This target reaction would transform heteroarene substructures, which are widely represented in drug discovery libraries,[17–19] into versatile heterocyclic α-amino acids with distinct biological properties.[20–22] Moreover, we envision that this dearomative transformation will enable rapid structural diversification along the newly installed molecular vector through the robust synthetic methodologies based around carboxylic acids.[23–27] This strategy could unlock access to large libraries of structurally diverse 3D heterocyclic molecules through iterative HTE hydrocarboxylation and diversification steps (Fig 1C).

Intermolecular indole hydrofunctionalization reactions remain limited despite the indole C2-C3 π-bond being prone to dearomative processes.[14,28–32] Established indole dearomative functionalization strategies rely on intramolecular nucleophiles or difunctionalization via delivery of two specific groups across the π-system.[12–16] Formal hydrocarboxylation of indole is currently accomplished via lithiation-

carboxylation-hydrogenation sequences, resulting in poor chemoselectivity that largely precludes implementation in complex settings. While recent work has introduced a collection of powerful metal-hydride-based alkene hydrocarboxylation reactions,[33,34] these approaches have been challenging to adapt to indole dearomatization.[35] We suspected that an alternative approach that exploits $CO_2^{\bullet-}$ as a key reactive intermediate would offer the requisite driving force to disrupt aromaticity and enable hydrocarboxylation of heteroaromatic systems. Pioneering work has introduced a variety of alkene hydrocarboxylation reactions that proceed through CO_2 reduction and subsequent addition of $CO_2^{\bullet-}$ to activated π-systems.[36–39] Unfortunately, this approach possesses two intrinsic challenges in the context of heteroarene hydrocarboxylation: (1) Chemoselectivity is limited due to the potent reductants required to reduce thermodynamically and kinetically stable CO_2;[40] (2) Dicarboxylation of the π-bond is a major liability as a result of the requisite CO_2 atmosphere.[41] Recent work from our group and others introduced a collection of photochemical approaches to generate $CO_2^{\bullet-}$ by abstracting a hydrogen atom from formate.[42–44] While this strategy has only been explored in the context of activated alkene hydrocarboxylation,[45,46] we questioned whether it could be adapted to the dearomative hydrocarboxylation of functionalized heteroarenes while retaining high chemoselectivity.

We launched our investigations by evaluating the reactivity of model *N*-acyl indole **1** under our previously reported conditions (Fig 1D).[45] While we obtained only poor conversion of our indole starting material, a low yield of the desired partially dearomatized indoline 2-carboxylic acid **2** was observed alongside the undesired dicarboxylated product **3** (2:1 ratio of **2**:**3**). Modestly increasing the loading of formate substantially improved reactivity; however, selectivity for the hydrofunctionalized product remained modest. We suspected that dicarboxylated product **3** could be formed via reduction of the benzylic radical intermediate followed by trapping with formate-derived CO_2 generated *in situ*. Consistent with this hypothesis, a significant increase in dicarboxylated product **3** was observed (1:2 ratio of **2**:**3**) when the reaction is conducted under a CO_2 atmosphere. Based on this observation, we questioned whether the addition of a small amount of water could introduce a mild proton source to outcompete CO_2

trapping. Indeed, the addition of two equivalents of water substantially increased the yield and eliminated undesired dicarboxylation products. Control experiments confirmed that no conversion of **1** was observed in the absence of photocatalyst or light.

With efficient indole hydrocarboxylation conditions in hand, we next evaluated the scope of this new method (Table 1). We found that both *N*-acyl (**3**) and *N*-Boc indole (**4**) underwent efficient carboxylation, while indoles bearing electron releasing N-substituents, such as methyl, were inert under the reaction conditions (see *Supporting Information* for details). The reaction is otherwise insensitive to indole electronics; substrates decorated with a variety of electron-donating and electron-withdrawing groups each underwent the desired transformation in high yields (**5**–**11**). These studies also revealed that dearomative hydrocarboxylation is favored over undesired side reactions at diverse medicinally relevant but potentially sensitive functional groups, such as carbamates (**4**, **11**), aryl fluorides (**5**), thioethers (**7**), amides (**9**, **20**, **24**–**26**), amines (**10**–**11**), pyridines (**12**–**16**, **18**, **19**), nitriles (**23**), and esters (**27**). Of note, substrates bearing coupling handles, such as aryl chlorides (**6**) and boron pinacol esters (**8**), could be transformed into the desired indoline carboxylic acid building blocks in high yield. Upon probing other heteroarene cores, we found that diverse azaindoles could be readily converted to the desired product (**12**–**16**). Hydrocarboxylation of more structurally distinct benzofuran (**17**), furopyridine (**18**, **19**), and isoquinolone (**20**) substructures similarly resulted in high yields of the dearomatized products in each case.

Next, we evaluated the effect of substitution at the reactive π-bond of the indole substrate. We found that C3-methyl indole was smoothly converted the desired product **21** with high diastereoselectivity for the trans isomer. Indole substrates substituted at the C3 position by a variety of different functional groups including arenes (**22**), nitriles (**23**), amides (**24**), and alkyl groups bearing diverse pendant functional groups (**25**–**27**) each underwent efficient and diastereoselective hydrocarboxylation.[47] Substitution at the site of $CO_2^{\bullet-}$ attack (C2) resulted in diminished reactivity; however, the desired product bearing a fully

Figure 2: Scope of dearomative hydrocarboxylation

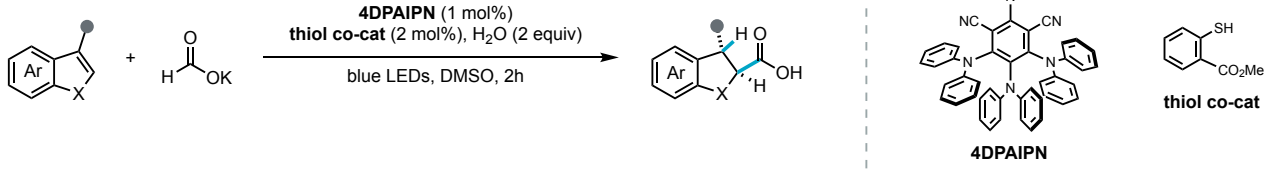

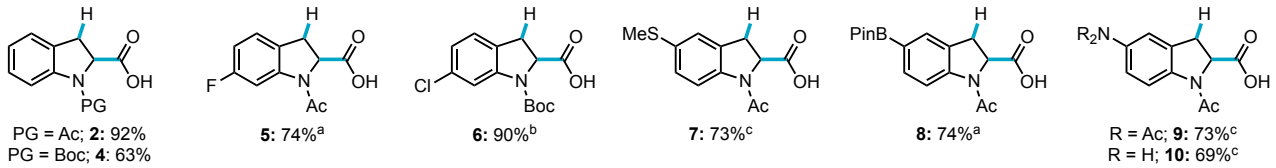

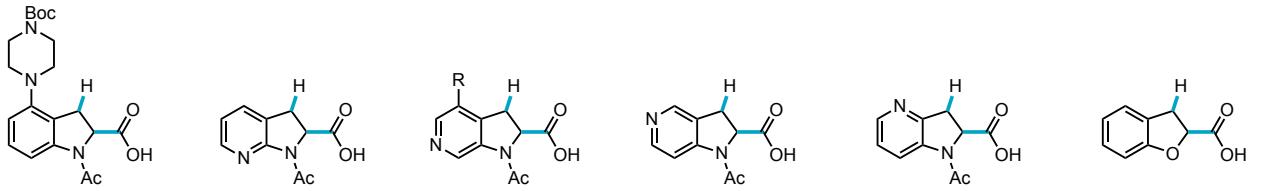

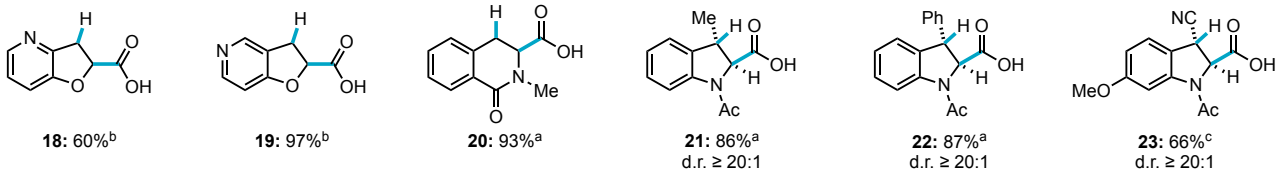

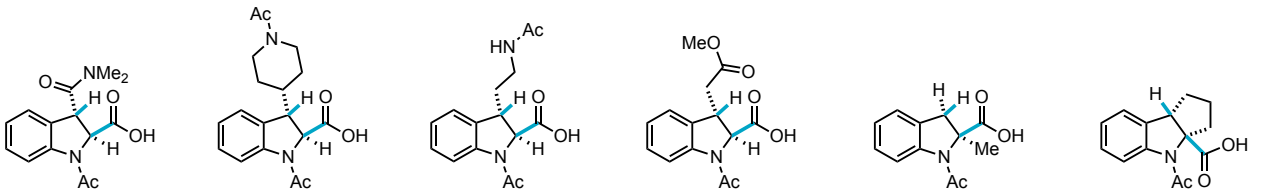

multigram scale in batch

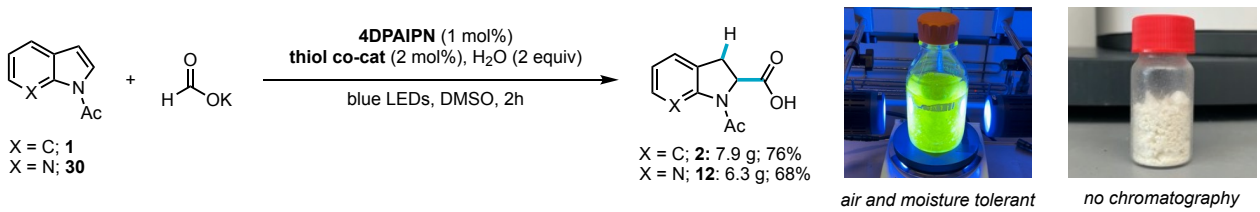

Reactions were conducted under air on a 0.5 mmol scale with 3 equiv $KCHO_2$ and yields are of purified product unless otherwise noted. See *Supporting Information* for further details. [a]Isolated as methyl ester after one-pot methylation procedure. [b]Yield determined by ^{1}H-NMR. [c]Isolated as ammonium carboxylate salt after purification. [d]Isolated as TFA salt after purification.

substituted carbon center (**28**) was nonetheless formed in sufficient quantities to enable early stage medicinal chemistry efforts. Furthermore, a tricyclic substrate bearing both C2 and C3 substitution underwent efficient hydrocarboxylation (**29**), presumably due to strain release upon radical addition. Taken together, these data highlight the complementarity of this new method relative to hydrogenation approaches that deliver exclusively cis-diastereomers and cannot generate products bearing fully substituted C2 positions.

Given the potential challenges scaling photochemical processes, we evaluated the efficiency of this new method in a preparative synthesis context. We found that hydrocarboxylation of both the initial model substrate (**1**) and a representative azaindole substrate (**30**) underwent efficient hydrocarboxylation on a multigram scale to deliver **2** and **12** each in high yield (>6 g of product in each case). These experiments illustrated three key practical assets of the reaction: (1) the reaction can be conducted preparatively using a conventional batch setup; (2) the reaction is robust and does not require any precautions to exclude air or moisture; (3) the products can be purified through precipitation or recrystallization without chromatography.

We next questioned whether this reaction could transform a library of molecules containing heterocyclic cores into more three-dimensionally complex analogs using HTE technology.[48] We selected a set of 48 heteroarene molecules of varying complexity ranging from building blocks to complex active pharmaceutical ingredients. These representative substrates were evaluated in quadruplicate using a microscale HTE format and a commercially available photoreactor. The desired α-amino acid products were obtained with high reproducibility in a 63% hit rate (using a threshold of 5% UPLC-MS assay yield). Three representative reactions were conducted on 0.2 mmol scale, unambiguously validating the identity of the desired amino acid products in each case (**31**–**33**). Taken together, these results illustrate how this method can be leveraged to rapidly prepare 3D analogs of more accessible planar heteroarene cores, even in a late-stage-functionalization setting.

Figure 3. HTE hydrocarboxylation to generate 3D building block libraries from 2D analogs

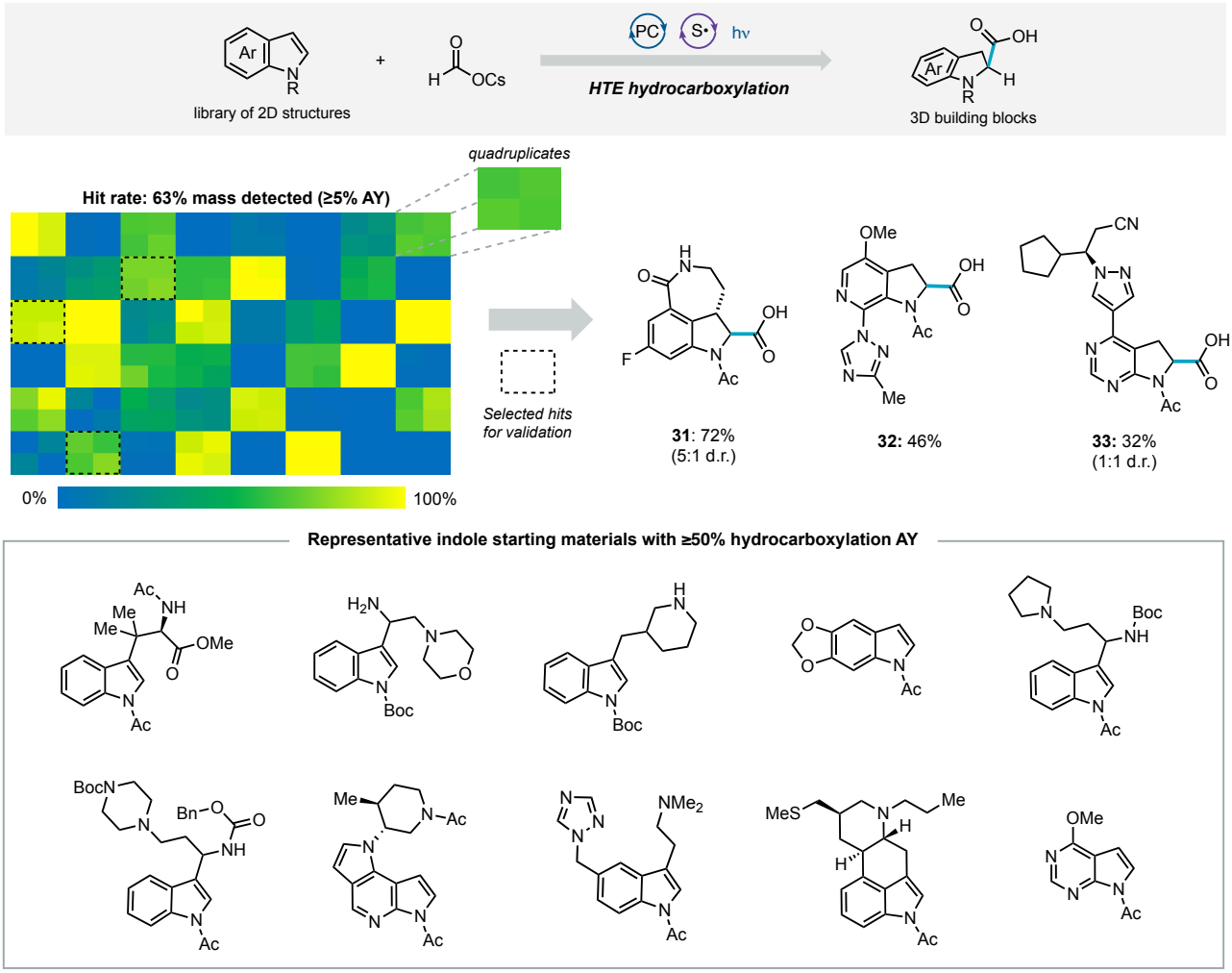

Reactions conducted on μmol scale using HTE well plates following otherwise standard conditions. UPLC-MS analysis of each reaction well used to ascertain whether the desired product is formed and estimate yield using the ratio of product over starting material absorbances (AY). Yields provided for **31**–**33** determined by 1H-NMR. See SI for details. AY = Assay Yield.

Given the well-established coupling reactions available to the carboxylic acid moiety, we envision that this new dearomative hydrocarboxylation reaction unlocks facile access to diverse 3D analogs from individual heteroarene lead compound or building blocks. As an illustrative proof-of-concept, we targeted HTE amidation given the ubiquity of amide bonds in pharmaceuticals and the structurally diverse array of readily available amines. To maximize coverage of medicinally-relevant chemical space, we conducted a two-step process[49] to select the targeted amine coupling partners from the Merck amine library (>17,000 compounds): (1)The initial library was strategically filtered down to amines that would result in ultimate amide products with druglike properties (see *Supporting Information* for details); (2) The resultant 6,286

Figure 4. Roadmap for high-throughput translation of indoles into diverse 3D analogs

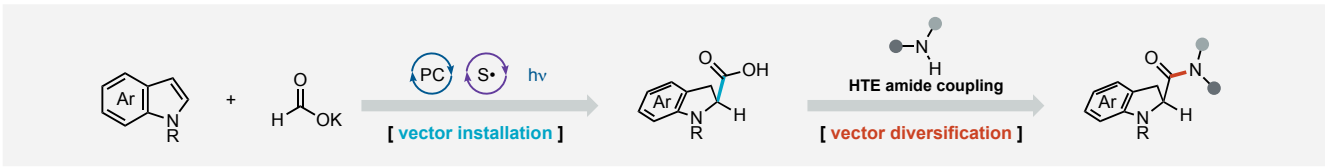

Amine selection process

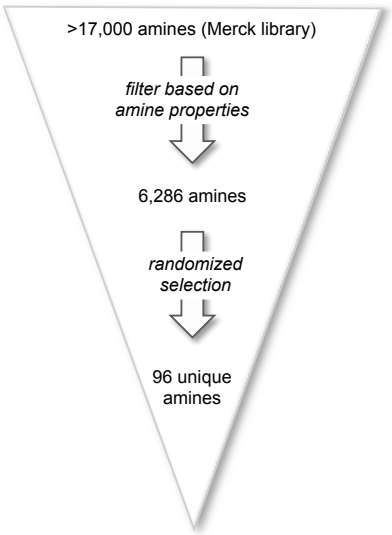

Visualization of chemical space coverage via t-SNE

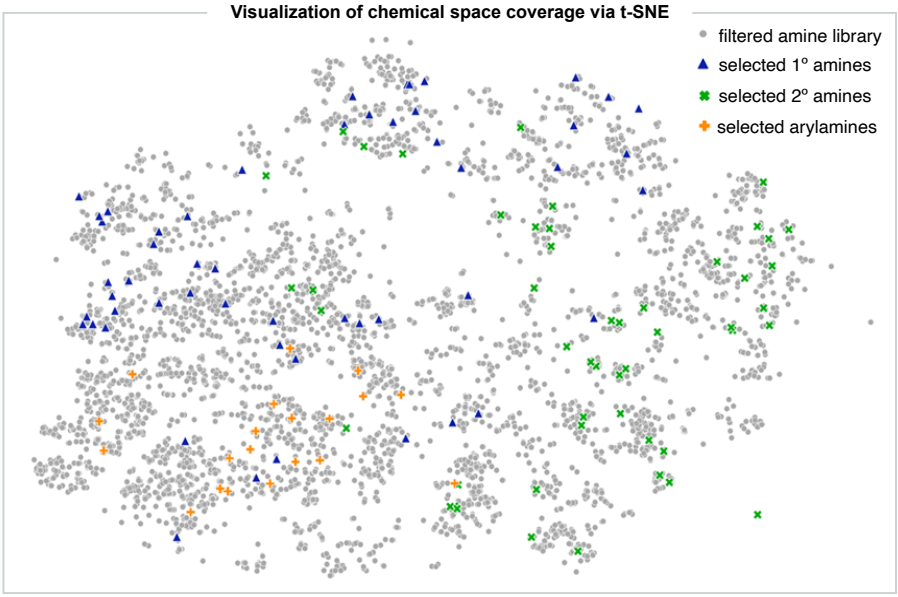

hit rate: 85% mass detected (≥5% AY)
(82 unique derivatives)

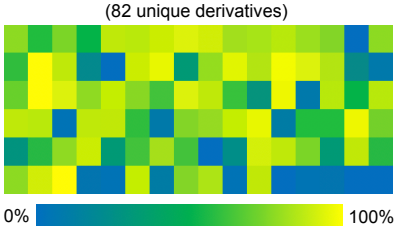

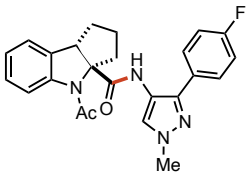

34: 65%

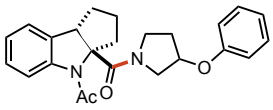

35: 63%

hit rate: 84% mass detected (≥5% AY)
(81 unique derivatives)

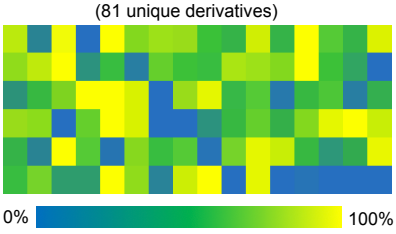

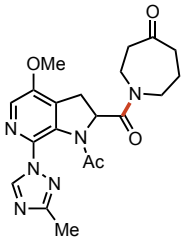

36: 74%

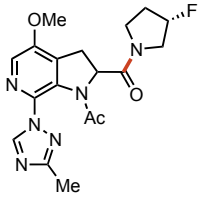

37: XX%

hit rate: 86% mass detected (≥5% AY)
(83 unique derivatives)

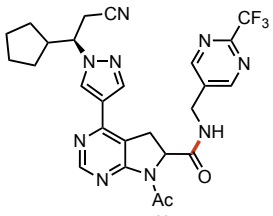

38: 63%

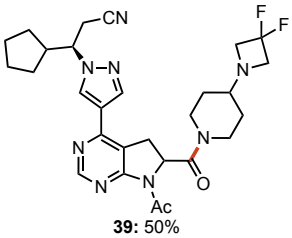

39: 50%

t-distributed stochastic neighbor embedding (t-SNE) plots of initially filtered amine set overlaid with the final selected monomers. The t-SNE plot visualizes 1024–bit, radius–2 molecular fingerprints in a 2D space. Amide couplings conducted on 1 μmol scale in HTE well plates under the following conditions: HATU (1.1 equiv), triethylamine (3 equiv), amine coupling partner (2.0 equiv) in DMF (0.1M) at 45°C for 16h. UPLC-MS analysis of each reaction well used to ascertain whether the desired product is formed and estimate yield using the ratio of product over starting material absorbances (AY). Validations yields provided for **34**–**39** determined by isolation following an amide coupling repeated on 0.5 mmol scale. See SI for details regarding amine selection process and experimental execution. AY = Assay Yield.

amine set was first randomly reduced to 130 coupling partners from which 96 amines were manually selected to allow for practical considerations such as availability. Broad coverage of amine chemical space was validated using t-distributed stochastic neighbor embedding (t-SNE) to visualize the molecular fingerprints of the selected amines overlaid with the initially filtered amine library.[50,51] The HTE amidation was conducted with a set of three indoline carboxylic acids representing both otherwise difficult-to-access building blocks (**29**) and complex cores for late-stage derivatization (**32**, **33**). This resulted in a hit rate of 84–86% across the three α-amino acid substrates (using a threshold of 5% UPLC-MS assay yield). This high-throughput diversification workflow illustrates how heteroarene hydrocarboxylation enables access to libraries of structurally diverse 3D molecules from readily accessible planar precursors.

Overall, we have developed a photocatalytic method for the dearomative hydrocarboxylation of heteroarenes. This reaction proceeds under mild conditions, allowing substrates bearing a wide variety of functional groups to undergo chemoselective hydrocarboxylation at the heteroarene subunit. Furthermore, C3-substituted indole substrates underwent a highly diastereoselective reaction, generating otherwise difficult-to-access *trans*-C2,C3-indoline products. This transformation can be directly employed in high-throughput derivatization as well as preparative synthesis on multigram scale. The generality and exquisite functional group tolerance of the reaction bodes well for adoption in late-stage functionalization of indole-based pharmaceutical leads. We envision this process introduces an ideal starting point to translate planar heterocycles into diverse 3D analogs through introduction of a single, readily manipulated molecular vector.

REFERENCES

1. Lovering, F., Bikker, J. & Humblet, C. Escape from Flatland: Increasing Saturation as an Approach to Improving Clinical Success. *J. Med. Chem.* **52**, 6752–6756 (2009).
2. Lovering, F. Escape from Flatland 2: complexity and promiscuity. *MedChemComm* **4**, 515–519 (2013).
3. Buskes, M. J. & Blanco, M.-J. Impact of Cross-Coupling Reactions in Drug Discovery and Development. *Molecules* **25**, 3493 (2020).
4. Schneider, N., Lowe, D. M., Sayle, R. A., Tarselli, M. A. & Landrum, G. A. Big Data from Pharmaceutical Patents: A Computational Analysis of Medicinal Chemists' Bread and Butter. *J. Med. Chem.* **59**, 4385–4402 (2016).
5. Ishikawa, M. & Hashimoto, Y. Improvement in Aqueous Solubility in Small Molecule Drug Discovery Programs by Disruption of Molecular Planarity and Symmetry. *J. Med. Chem.* **54**, 1539–1554 (2011).
6. Huck, C. J. & Sarlah, D. Shaping Molecular Landscapes: Recent Advances, Opportunities, and Challenges in Dearomatization. *Chem* **6**, 1589–1603 (2020).
7. Pape, A. R., Kaliappan, K. P. & Kündig, E. P. Transition-Metal-Mediated Dearomatization Reactions. *Chem. Rev.* **100**, 2917–2940 (2000).
8. Roche, S. P. & Porco Jr., J. A. Dearomatization Strategies in the Synthesis of Complex Natural Products. *Angew. Chem. Int. Ed.* **50**, 4068–4093 (2011).
9. Recent developments in enantio- and diastereoselective hydrogenation of N-heteroaromatic compounds. *Org. Biomol. Chem.* **20**, 1794–1827 (2022).
10. Kim, A. N. & Stoltz, B. M. Recent Advances in Homogeneous Catalysts for the Asymmetric Hydrogenation of Heteroarenes. *ACS Catal.* **10**, 13834–13851 (2020).

11. Wiesenfeldt, M. P., Nairoukh, Z., Dalton, T. & Glorius, F. Selective Arene Hydrogenation for Direct Access to Saturated Carbo- and Heterocycles. *Angew. Chem. Int. Ed.* **58**, 10460–10476 (2019).
12. Zhu, M., Zhang, X., Zheng, C. & You, S.-L. Energy-Transfer-Enabled Dearomative Cycloaddition Reactions of Indoles/Pyrroles via Excited-State Aromatics. *Acc. Chem. Res.* **55**, 2510–2525 (2022).
13. Zheng, C. & You, S.-L. Advances in Catalytic Asymmetric Dearomatization. *ACS Cent. Sci.* **7**, 432–444 (2021).
14. Abou-Hamdan, H., Kouklovsky, C. & Vincent, G. Dearomatization Reactions of Indoles to Access 3D Indoline Structures. *Synlett* **31**, 1775–1788 (2020).
15. James, M. J., O'Brien, P., Taylor, R. J. K. & Unsworth, W. P. Synthesis of Spirocyclic Indolenines. *Chem. – Eur. J.* **22**, 2856–2881 (2016).
16. Roche, S. P., Youte Tendoung, J.-J. & Tréguier, B. Advances in dearomatization strategies of indoles. *Tetrahedron* **71**, 3549–3591 (2015).
17. Vitaku, E., Smith, D. T. & Njardarson, J. T. Analysis of the Structural Diversity, Substitution Patterns, and Frequency of Nitrogen Heterocycles among U.S. FDA Approved Pharmaceuticals. *J. Med. Chem.* **57**, 10257–10274 (2014).
18. Meanwell, N. A. Chapter Five - A Synopsis of the Properties and Applications of Heteroaromatic Rings in Medicinal Chemistry. in *Advances in Heterocyclic Chemistry* (eds. Scriven, E. F. V. & Ramsden, C. A.) vol. 123 245–361 (Academic Press, 2017).
19. Heravi, M. M. & Zadsirjan, V. Prescribed drugs containing nitrogen heterocycles: an overview. *RSC Adv.* **10**, 44247–44311 (2020).
20. Ontoria, J. M. *et al.* The Design and Enzyme-Bound Crystal Structure of Indoline Based Peptidomimetic Inhibitors of Hepatitis C Virus NS3 Protease. *J. Med. Chem.* **47**, 6443–6446 (2004).
21. Gruenfeld, N. *et al.* Angiotensin converting enzyme inhibitors: 1-glutarylindoline-2-carboxylic acid derivatives. *J. Med. Chem.* **26**, 1277–1282 (1983).

22. Bohacek, R., De Lombaert, S., McMartin, C., Priestle, J. & Grütter, M. Three-Dimensional Models of ACE and NEP Inhibitors and Their Use in the Design of Potent Dual ACE/NEP Inhibitors. *J. Am. Chem. Soc.* **118**, 8231–8249 (1996).

23. Lanigan, R. M. & Sheppard, T. D. Recent Developments in Amide Synthesis: Direct Amidation of Carboxylic Acids and Transamidation Reactions. *Eur. J. Org. Chem.* **2013**, 7453–7465 (2013).

24. Beil, S. B., Chen, T. Q., Intermaggio, N. E. & MacMillan, D. W. C. Carboxylic Acids as Adaptive Functional Groups in Metallaphotoredox Catalysis. *Acc. Chem. Res.* **55**, 3481–3494 (2022).

25. Patra, T. & Maiti, D. Decarboxylation as the Key Step in C–C Bond-Forming Reactions. *Chem. – Eur. J.* **23**, 7382–7401 (2017).

26. Rodríguez, N. & Goossen, L. J. Decarboxylative coupling reactions: a modern strategy for C–C-bond formation. *Chem. Soc. Rev.* **40**, 5030–5048 (2011).

27. Laudadio, G., Palkowitz, M. D., El-Hayek Ewing, T. & Baran, P. S. Decarboxylative Cross-Coupling: A Radical Tool in Medicinal Chemistry. *ACS Med. Chem. Lett.* **13**, 1413–1420 (2022).

28. Alam, R., Diner, C., Jonker, S., Eriksson, L. & Szabó, K. J. Catalytic Asymmetric Allylboration of Indoles and Dihydroisoquinolines with Allylboronic Acids: Stereodivergent Synthesis of up to Three Contiguous Stereocenters. *Angew. Chem. Int. Ed.* **55**, 14417–14421 (2016).

29. Beaud, R., Guillot, R., Kouklovsky, C. & Vincent, G. FeCl3-Mediated Friedel–Crafts Hydroarylation with Electrophilic N-Acetyl Indoles for the Synthesis of Benzofuroindolines. *Angew. Chem. Int. Ed.* **51**, 12546–12550 (2012).

30. Morimoto, N., Morioku, K., Suzuki, H., Takeuchi, Y. & Nishina, Y. Lewis Acid and Fluoroalcohol Mediated Nucleophilic Addition to the C2 Position of Indoles. *Org. Lett.* **18**, 2020–2023 (2016).

31. Bubnov, Y. N., Zhun', I. V., Klimkina, E. V., Ignatenko, A. V. & Starikova, Z. A. Reductive 1,2-Allylboration of Indoles by Triallyl- and Triprenylborane – Synthesis of 2-Allylated Indolines. *Eur. J. Org. Chem.* **2000**, 3323–3327 (2000).

32. Nowrouzi, F. & Batey, R. A. Regio- and Stereoselective Allylation and Crotylation of Indoles at C2 Through the Use of Potassium Organotrifluoroborate Salts. *Angew. Chem. Int. Ed.* **52**, 892–895 (2013).

33. Davies, J., Lyonnet, J. R., Zimin, D. P. & Martin, R. The road to industrialization of fine chemical carboxylation reactions. *Chem* **7**, 2927–2942 (2021).

34. Liu, Q., Wu, L., Jackstell, R. & Beller, M. Using carbon dioxide as a building block in organic synthesis. *Nat. Commun.* **6**, 5933 (2015).

35. Liu, K., Song, Y.-F., Gao, Y., Luo, J.-Q. & Jia, Y.-X. NiH-catalyzed dearomative hydroalkylation of indoles. *Chem. Commun.* **58**, 5893–5896 (2022).

36. Alkayal, A. *et al*. Harnessing Applied Potential: Selective β-Hydrocarboxylation of Substituted Olefins. *J. Am. Chem. Soc.* **142**, 1780–1785 (2020).

37. Seo, H., Liu, A. & Jamison, T. F. Direct β-Selective Hydrocarboxylation of Styrenes with CO2 Enabled by Continuous Flow Photoredox Catalysis. *J. Am. Chem. Soc.* **139**, 13969–13972 (2017).

38. Kang, G. & Romo, D. Photocatalyzed, β-Selective Hydrocarboxylation of α,β-Unsaturated Esters with CO2 under Flow for β-Lactone Synthesis. *ACS Catal.* **11**, 1309–1315 (2021).

39. Huang, H. *et al*. Visible-Light-Driven Anti-Markovnikov Hydrocarboxylation of Acrylates and Styrenes with CO2. *CCS Chem.* **3**, 1746–1756 (2020).

40. Gennaro, A., Isse, A. A., Savéant, J.-M., Severin, M.-G. & Vianello, E. Homogeneous Electron Transfer Catalysis of the Electrochemical Reduction of Carbon Dioxide. Do Aromatic Anion Radicals React in an Outer-Sphere Manner? *J. Am. Chem. Soc.* **118**, 7190–7196 (1996).

41. You, Y. *et al*. Electrochemical Dearomative Dicarboxylation of Heterocycles with Highly Negative Reduction Potentials. *J. Am. Chem. Soc.* **144**, 3685–3695 (2022).

42. Wang, H., Gao, Y., Zhou, C. & Li, G. Visible-Light-Driven Reductive Carboarylation of Styrenes with CO2 and Aryl Halides. *J. Am. Chem. Soc.* **142**, 8122–8129 (2020).

43. Hendy, C. M., Smith, G. C., Xu, Z., Lian, T. & Jui, N. T. Radical Chain Reduction via Carbon Dioxide Radical Anion (CO2•–). *J. Am. Chem. Soc.* **143**, 8987–8992 (2021).

44. Chmiel, A. F., Williams, O. P., Chernowsky, C. P., Yeung, C. S. & Wickens, Z. K. Non-innocent Radical Ion Intermediates in Photoredox Catalysis: Parallel Reduction Modes Enable Coupling of Diverse Aryl Chlorides. *J. Am. Chem. Soc.* **143**, 10882–10889 (2021).

45. Alektiar, S. N. & Wickens, Z. K. Photoinduced Hydrocarboxylation via Thiol-Catalyzed Delivery of Formate Across Activated Alkenes. *J. Am. Chem. Soc.* **143**, 13022–13028 (2021).

46. Huang, Y. *et al*. Photoredox Activation of Formate Salts: Hydrocarboxylation of Alkenes via Carboxyl Group Transfer. *ACS Catal.* **11**, 15004–15012 (2021).

47. In some cases, lower diastereoselectivity was observed in the crude reaction mixture but the diastereoselectivity increased upon purification. Based on a mass balance assessment we suspect this a consequence of isomerization rather than purification. See Supporting Information for details.

48. Buitrago Santanilla, A. *et al*. Nanomole-scale high-throughput chemistry for the synthesis of complex molecules. *Science* **347**, 49–53 (2015).

49. Xu, J. *et al*. Roadmap to Pharmaceutically Relevant Reactivity Models Leveraging High-Throughput Experimentation. Preprint at https://doi.org/10.26434/chemrxiv-2022-x694w (2022).

50. Maaten, L. van der & Hinton, G. Visualizing Data using t-SNE. *J. Mach. Learn. Res.* **9**, 2579–2605 (2008).

51. S. Kutchukian, P. *et al*. Chemistry informer libraries: a chemoinformatics enabled approach to evaluate and advance synthetic methods. *Chem. Sci.* **7**, 2604–2613 (2016).

AUTHOR INFORMATION

Corresponding Author

* Zachary K. Wickens (wickens@wisc.edu)

* Charles Yeung (charles.yeung@merck.com)

Author Contributions

The manuscript was written through contributions of all authors. The experiments were designed through contributions of all authors. MM and SNA conducted all experiments. All authors have given approval to the final version of the manuscript.

ACKNOWLEDGMENT

We thank the Postdoctoral Research Program of Merck Sharp & Dohme LLC, a subsidiary of Merck & Co., Inc., Rahway, NJ, USA for its generous support of M.C.L. and the work disclosed in this manuscript. We thank Nunzio Sciammetta for his support and guidance throughout the duration of this project. We thank Lisa M. Nogle, David A. Smith, Adam Beard, Miroslawa Darlak, Spencer McMinn, Yingchun Ye, and Mark Pietrafitta for reversed-phase purifications (Merck & Co., Inc., Rahway, NJ, USA). We thank Pablo Trigo Mouriño and Samantha Anne Burgess for their help with NMR structure elucidation and Wilfredo Pinto for the HRMS data analysis (Merck & Co., Inc., Rahway, NJ, USA). We acknowledge Thomas Struble for his work on python script for randomized selection and t-SNE plot (Merck & Co., Inc., Rahway, NJ, USA), and Dipannita Kalyani for her guidance with amine filtration (Merck & Co., Inc., Rahway, NJ, USA). We thank Ron Ferguson, Kevin D. Dykstra, Mycah Uehling, Michael Wleklinski, and Maria-Elena Liosi for their insights on HTE instrumentation and execution, and Mufeda Zhort for HTE UPLC-MS data acquisition (Merck & Co., Inc., Rahway, NJ, USA).This work was supported by funding from the NIH (1R01GM146063-01).